The International Journal of Cardiovascular Imaging (2019) 35:955–964
https://doi.org/10.1007/s10554-018-01514-4

ORIGINAL PAPER

Adjustment of vascular 2-deoxy-2-[^{18}F]fluoro-D-glucose uptake values over time through a modeling approach

Pavlos P. Kafouris[1,2] · Iosif P. Koutagiar[3] · Alexandros T. Georgakopoulos[2] · Nikoletta K. Pianou[2] · Marinos G. Metaxas[2] · George M. Spyrou[4] · Constantinos D. Anagnostopoulos[2]

Received: 26 September 2018 / Accepted: 15 December 2018 / Published online: 31 January 2019

Abstract

To develop and test a model predicting 2-deoxy-2-[^{18}F]fluoro-D-glucose ([^{18}F]FDG) standardized uptake value (SUV) changes over time in the aorta and the superior vena cava (SVC). Maximum aortic SUV and mean SVC SUV were determined at two time points (T1 and T2) in the ascending (ASC), descending (DSC), abdominal (ABD) aorta, aortic arch (ARC) and SVC of patients who have undergone [^{18}F]FDG PET/CT for clinical purposes. For SUV prediction at T2, linear and non-linear models of SUV difference for a given time change were developed in a derivation group. The results were tested in an independent validation group, whilst model reproducibility was tested in patients of the validation group who have undergone a second clinically indicated scan. Applying the linear model in the derivation group, there were no statistically significant differences in measurements obtained in the examined segments: mean differences ranged from 0 ± 0.10 in SVC to 0.01 ± 0.13 in ARC between measured and predicted SUV. In contrast, in the non-linear model, there were statistically significant differences in measurements, except in ARC, with mean differences ranging from 0.04 ± 0.14 in ARC to 0.28 ± 0.13 in ABD. In the validation group using the linear model, there were no statistically significant differences, with mean differences ranging from -0.01 ± 0.08 in ASC to -0.03 ± 0.11 in ABD. Regarding reproducibility, mean differences were no statistically significant, ranging from 0.004 ± 0.06 in ASC to -0.02 ± 0.16 in ABD. We have developed a linear model allowing accurate and reproducible prediction of SUV changes over time in the aorta and SVC.

Keywords Standardized uptake value · [^{18}F]FDG · PET/CT · Circulation time · Cardiovascular imaging · Delayed imaging

Introduction

Positron emission tomography (PET)/computed tomography (CT) with 2-deoxy-2-[^{18}F]fluoro-D-glucose ([^{18}F]FDG) is a promising technique for detecting, locating and quantifying the presence of inflammatory activation within the wall of carotid, aorta and coronary arteries [1–4]. There are several methods for measuring [^{18}F]FDG uptake in the vascular tree. The most common index of uptake quantification is the standardized uptake value (SUV) normalized using either the body weight, the lean body mass or the body surface area [5]. SUV depends on numerous factors including patient weight, plasma glucose level, partial-volume effects, recovery coefficient, type of regions of interest (ROI), number of iterations used for reconstruction and the post-filtering applied to reconstructed images and circulation time (the time interval between [^{18}F]FDG injection and starting time of data acquisition) [5–7]. Regarding the latter, current guidelines [8] recommend an uptake time of 60 min for oncology studies, however, for arterial PET imaging, longer circulation times (2–3 h post injection) are recommended to allow sufficient [^{18}F]FDG accumulation in the arterial wall and to reduce the noise from the [^{18}F]FDG uptake in the blood pool [9].

✉ Constantinos D. Anagnostopoulos
cdanagnostopoulos@bioacademy.gr

1 Department of Informatics and Telecommunications, National and Kapodistrian University of Athens, Athens, Greece

2 Experimental Surgery, Clinical and Translational Research Centre, Biomedical Research Foundation of the Academy of Athens, Athens, Greece

3 First Department of Cardiology, Hippokration Hospital, Athens, Greece

4 Bioinformatics ERA Chair, The Cyprus Institute of Neurology and Genetics, Nicosia, Cyprus

Prior studies have shown that in breast [10, 11] and lung [12] cancer, SUV can be predicted at a specific time interval by a linear model. We hypothesize that such prediction is also feasible for SUV in the vascular tree. Thus, the aim of the current study was to develop and test models predicting SUV changes over time for several vascular segments.

Materials and methods

Study population

Following approval of the medical research and ethics committee of our Institute, 45 patients who have undergone [^{18}F]FDG PET/CT imaging between April 2015 and January 2018 for clinical purposes and found to be free of malignant or inflammatory disease at the time of scanning were enrolled in the present study. For the purposes of creation of a predictive model describing the SUV change over time, a derivation and a separate validation group of individuals free of disease were constructed. In agreement with prior studies, 2/3 (or 60–70%) of subjects comprised the derivation set and the rest 1/3 (or 40–30%) the validation set [13, 14]. Specifically, patients scanned from April 2015 to July 2016 formed the derivation cohort (30 patients), whilst patients scanned from August 2016 to June 2017 formed the validation cohort. For testing the reproducibility of our model, vascular SUV changes over time were tested twice in the first 6 patients from the validation group who have undergone a second scan (interval: 127.56 ± 55.68 days) for clinical purposes (surveillance scan in patients with treated lymphoproliferative disease) and continued to be disease-free. An identical imaging and processing protocol was used in the derivation and validation groups.

[^{18}F]FDG PET/CT imaging

[^{18}F]FDG PET/CT imaging was performed after a period of at least 6-h fasting. Plasma glucose levels were < 180 mg/dL. Images were obtained after intravenous administration of 140 μCi/kg [^{18}F]FDG (Biocosmos S.A., Greece). Whole body [^{18}F]FDG PET/CT imaging (Biograph 6; Siemens, Forchheim) was performed for clinical purposes with the patient placed in supine position, as per current recommendations at around 60 min post injection [8]. For measuring SUV in the thoracic and abdominal aorta, delayed imaging of the thorax and abdomen was also performed in all subjects. A low-dose, non-gated, non-contrast-enhanced CT was obtained before the PET scan on both the early and the delayed studies, for attenuation correction and anatomic localization. The acquisition parameters were as follows: 30 mA, 110 KV, and axial slice thickness of 1.25 mm. PET images were reconstructed using a standard ordered-subset expectation maximization algorithm with the following reconstruction parameters: three iterations and eight subsets.

[^{18}F]FDG uptake measurements

[^{18}F]FDG PET/CT studies were assessed without knowledge of patients' clinical data, by 3 independent readers (IK, PK and AG) with experience in analysis of vascular PET/CT images [15, 16]. Datasets from the derivation group were assessed by IK, those from the validation group by PK, while those from the reproducibility group by AG. To minimize patients' exposure to radiation from a second CT scan and reduce the influence of partial volume effect that could have affected the testing and validation of the predictive model, we did not assess [^{18}F]FDG uptake in the carotid arteries and therefore, measurements were obtained only in the following aortic segments: ascending aorta (ASC), aortic arch (ARC), descending (DSC) and abdominal aorta (ABD) and also in the superior vena cava (SVC). ROIs around the arterial wall were manually drawn along the whole vessel in consecutive axial images at intervals of 5 mm for the thoracic and ABD. [^{18}F]FDG uptake was measured by SUV which is defined as a ratio of tissue radioactivity concentration at time t, $C_{PET}(t)$, and administered dose at the time of injection divided by body weight. Tissue radioactivity and dose was decay-corrected to the same time point. Thus,

$$\mathrm{SUV} = C_{PET}(t) / \left[\mathrm{Dose}/\mathrm{Weight}\right] \quad (1)$$

For [^{18}F]FDG uptake quantification, SUVmax (maximum SUV based on body weight) was recorded as the highest pixel activity within the ROI. By averaging the SUVmax among the slices of each aortic segment, we derived a mean SUVmax value for the entire segment. For assessing [^{18}F]FDG changes over time in SVC, a structure that is commonly used for correcting arterial uptake from blood activity, 6 circular ROIs 3 to 4 mm diameter at least were placed over the SVC.

Subsequently, the average SUV computed within a ROI produced a reliable estimate of the mean SUV for each segment, which is defined here as SUVmean (used for SVC measurements only). The same procedure was followed both in the early (T1) and late (T2) scans. Therefore, for all patients, the difference of SUVmax or SUVmean in T1 and T2 ($\Delta\mathrm{SUVmax} = \mathrm{SUVmax}^{T2} - \mathrm{SUVmax}^{T1}$ or $\Delta\mathrm{SUVmean} = \mathrm{SUVmean}^{T2} - \mathrm{SUVmean}^{T1}$ respectively) was calculated in each of the arterial segments and the SVC. Consequently, for each subject the difference time between the two scans ($\Delta T = T2 - T1$) and the ΔSUV (ΔSUVmax or ΔSUVmean) of each vascular segment were evaluated. From now on, the term SUV will stand for SUVmax for all the aortic segments (ASC, ARC, DSC and ABD) and SUVmean for the SVC.

Model development

The prediction of SUV at different time points was performed by developing models relating the difference in SUV (ΔSUV) for a given change in time (ΔT) for each examined segment. A linear and a non-linear model were developed and then we performed a comparison between these models regarding their ability to predict accurately delayed SUVs. Figure 1 shows the lines through the 2 points: (T1, SUV^{T1}) and (T2, SUV^{T2}) for each examined segment and for each patient. In agreement with prior studies demonstrating a reduction of arterial SUV over time [17, 18], a predictive model was developed based on confirmation of SUV reduction at T2 compared to T1.

By collecting the pairs (ΔT, ΔSUV) from each patient and for all aortic segments, we investigated the "optimal" line/curve which fits better to the points (ΔT, ΔSUV). Therefore, a predictive model was constructed for each of the five segments of interest. Considering the variability of SUV between studies in the same patient [5–7, 19, 20], we have tried to introduce this variability by simulating SUV values within a broader range for all the SUV measurements in both times (T1, T2). This procedure was accomplished by the random sampling Monte Carlo Inversion Technique [21]. Specifically, we populated our sample by generating 1000 (ΔT, $\widetilde{\Delta SUV}$) points (*patients)* for each arterial segment, which differ ± 10% maximum from the actual measurements (ΔT, ΔSUV) of the patients we measured. These points were subjected to two basic constraints: (i) SUV^{T1} should always be ≥ SUV^{T2} in all five segments, (ii) the line, which fits better the (ΔT, $\widetilde{\Delta SUV}$) points was used after their generation and filtering according to the first constraint. Thus, after calculation of $\widetilde{\Delta SUV}$ of the examined segment, the "optimal" line was found for each segment. However, if the line had positive slope the line was rejected, because as ΔT increases, ΔSUV should be decreased. The final representative line was derived by averaging a large number of lines (< 1000) satisfying the above limitations for each segment of interest.

Eighteen patients were randomly selected from the derivation group to define the training set and the remaining twelve comprised the test set. The final line for each arterial segment (ASC, ARC, DSC and ABD) and SVC was calculated based on the procedure described above. The predicted value of SUV at time T2 ($\widetilde{SUV}^{T2}$) was derived from this line for each of the patients of the test-set and for each segment. Subsequently, the prediction's error was computed by subtracting the predicted value ($\widetilde{SUV}^{T2}$) from the measured (SUV^{T2}) ($error_{SUV^{T2}} = SUV^{T2} - \widetilde{SUV}^{T2}$) along with its mean value ($mean_{error}$) and the corresponding standard deviation (SD_{error}).

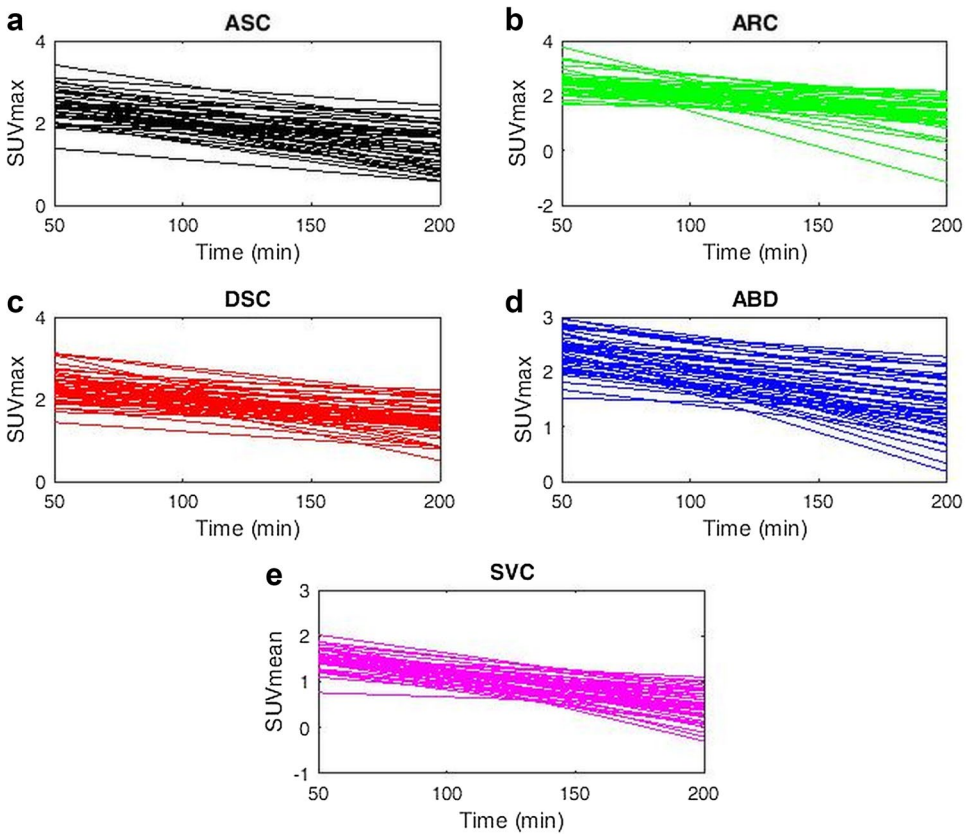

Fig. 1 The lines through the 2 points: (T1, SUV^{T1}) and (T2, SUV^{T2}) for each examined segment and patient. SUV decreases over time in interval [50, 170] min in **a** ASC, **b** ARC, **c** DSC, **d** ABD and **e** SVC in our patients. *SUV* indicates standardized uptake value, *ASC* ascending aorta, *ARC* aortic arch, *DSC* descending aorta, *ABD* abdominal aorta, *SVC* superior vena cava

Finally, the following score was calculated to rank better the cases where the mean value and the variance of the prediction's error were simultaneously small:

$$\text{score}_{\text{error}} = \left|\text{mean}_{\text{error}} \times \text{SD}_{\text{error}}\right| \quad (2)$$

We repeated this procedure by shuffling our data and creating 100 different pairs of training/test sets keeping always the same proportion. The best line for each segment was selected to be the one that had the minimum value of the $\text{score}_{\text{error}}$.

Linear model

Assuming a linear reduction in SUV over time (approximately at [50–170] min), as mentioned above, the relationship between ΔSUV and ΔT will be:

$$\begin{aligned} &\Delta\text{SUV} = \alpha * \Delta\text{T} + \text{b} \Leftrightarrow \\ &\widetilde{\text{SUV}}^{\text{T2}} = \text{SUV}^{\text{T1}} + \alpha * (\text{T2} - \text{T1}) + \text{b} \end{aligned} \quad (3)$$

where $\widetilde{\text{SUV}}^{\text{T2}}$ is the estimated SUV at a desired time T2, SUV^{T1} is the measured SUV at time T1, α is the slope of the line and b is the y-intercept. The line must have negative slope, that is $\alpha < 0$.

Non-linear model

We have also attempted to develop a non-linear model to examine, which model presents the best predictive ability. The same constraints as in the case of the linear model were applied. Accordingly, we presumed that the non-linear model describing the relationship of the ΔSUV with the ΔT should be represented with the power function: $y = a * x^b$ for all the segments of interest. Therefore, the prediction of SUV derived from the equation:

$$\begin{aligned} &\Delta\text{SUV} = \alpha * \Delta\text{T}^{\text{b}} \Leftrightarrow \\ &\widetilde{\text{SUV}}^{\text{T2}} = \text{SUV}^{\text{T1}} + \alpha * (\text{T2} - \text{T1})^{\text{b}} \end{aligned} \quad (4)$$

where α, b are constants. The best curve for each segment was derived following the same procedure used for the linear model.

Statistical analysis

For comparisons between measurements in the derivation and the validation group, quantitative data are presented as mean values ± standard deviation. Jarque–Bera and Lilliefors tests were used to test for a normal distribution, and a two-sample F-test for equal variances. Mean differences between groups were assessed using the two-sample t-test for continuous variables. For non-continuous variables, Fisher's exact test was employed. Pearson's correlation coefficients were used to test the relationship between measured and predicted SUVs. A value of $p < 0.05$ was considered significant. Statistical analysis was performed with commercially available software (Version 9.2; Matlab R2017a).

Results

The characteristics of the study population are summarized in Table 1. The best lines/curves and consequently the final values of the α, b variables for the segments of interest are displayed in Tables 2 and 3 (linear and non-linear model respectively). In addition, the corresponding lines are displayed in Figs. 2 and 3.

Differences between measured and predicted SUVs

The measured (ΔSUV) and predictive ($\widetilde{\Delta\text{SUV}}$) measurements in the derivation group are depicted in Table 4. Using a linear model, mean difference between measured and predicted SUV in the examined vascular segments was: 0.01 ± 0.11 (p = 0.66) for ASC, 0.01 ± 0.13 (p = 0.90)

Table 1 Study population

	Derivation group (n = 30)	Validation group (n = 15)	p
Age (years)	56 ± 19.13	62.73 ± 14.68	0.15
Male gender	22 (73.3%)	13 (86.6%)	0.46
Weight (Kg)	79.73 ± 17.62	77.13 ± 10.44	0.60
Glucose (mg/dL)	110.13 ± 22.31	105.93 ± 24.16	0.57
T1 (min)	69.66 ± 8.72	65.87 ± 9.33	0.18
$\text{SUVmax}^{\text{T1}}$	2.29 ± 0.36	2.24 ± 0.32	0.38
$\text{SUVmean}^{\text{T1}}$	1.36 ± 0.17	1.44 ± 0.29	0.27
T2 (min)	132.29 ± 18.80	129.11 ± 22.59	0.62
$\text{SUVmax}^{\text{T2}}$	1.90 ± 0.30	1.83 ± 0.33	0.19
$\text{SUVmean}^{\text{T2}}$	0.97 ± 0.17	1.00 ± 0.22	0.56

All values are expressed as mean ± SD or n (%)

$SUVmax^{T1\ (or\ T2)}$ indicates maximum standardized uptake value at T1 (or T2), $SUVmean^{T1\ (or\ T2)}$ mean standardized uptake value at T1 (or T2)

Table 2 Final values of α, b for each segment and factors characterizing the prediction's error according to the linear model

Segment	Slope (a)	Intercept (b)	$Mean_{error}$	SD_{error}	$Score_{error}$
ASC	−0.0035	−0.1750	−0.0006	0.1263	0.00008
ARC	−0.0013	−0.3903	−0.0010	0.2760	0.00028
DSC	−0.0040	−0.1016	−0.0003	0.1470	0.00004
ABD	−0.0036	−0.1562	−0.0029	0.1440	0.00042
SVC	−0.0041	−0.1352	−0.0003	0.1228	0.00004

ASC indicates ascending aorta, *ARC* aortic arch, *DSC* descending aorta, *ABD* abdominal aorta, *SVC* superior vena cava, $mean_{error}$ mean value of prediction's error computed by subtracting the predicted value ($\widetilde{SUV}^{T2}$) from the measured (SUV^{T2}), SD_{error} standard deviation of prediction's error, $score_{error} = |mean_{error} \times SD_{error}|$

Table 3 Final values of α, b for each segment and factors characterizing the prediction's error according to the non-linear model

Segment	a	b	$Mean_{error}$	SD_{error}	$Score_{error}$
ASC	−0.1293	0.3533	0.1222	0.0832	0.0102
ARC	−0.2648	0.1553	−0.0104	0.3008	0.0031
DSC	−0.0849	0.4403	0.1413	0.1243	0.0176
ABD	−0.0754	0.5232	0.2914	0.0600	0.0175
SVC	−0.0384	0.6070	0.0438	0.0979	0.0043

ASC indicates ascending aorta, *ARC* aortic arch, *DSC* descending aorta, *ABD* abdominal aorta, *SVC* superior vena cava, *a and b* constants of the non-linear model, $mean_{error}$ mean value of prediction's error computed by subtracting the predicted value ($\widetilde{SUV}^{T2}$) from the measured (SUV^{T2}), SD_{error} standard deviation of prediction's error, $score_{error} = |mean_{error} \times SD_{error}|$

for ARC, 0.01 ± 0.12 (p = 0.67) for DSC, 0.01 ± 0.12 (p = 0.67) for ABD and 0 ± 0.10 (p = 0.96) for SVC, while in the non-linear model, 0.17 ± 0.13 (p < 0.05) for ASC, 0.04 ± 0.14 (p = 0.49) for ARC, 0.18 ± 0.12 (p < 0.05) for DSC, 0.28 ± 0.13 (p < 0.05) for ABD and 0.08 ± 0.15 (p < 0.05) for SVC. Subsequently, because of the observed statistically significant differences between actual and predicted measurements, only the linear model was tested in a validation group.

Validation study

In the linear model, mean difference between measured and predicted SUVs in the examined vascular segments was: -0.01 ± 0.08 (p = 0.72) for ASC, 0.02 ± 0.11 (p = 0.56) for ARC, 0.03 ± 0.10 (p = 0.33) for DSC, -0.03 ± 0.11 (p = 0.34) for ABD and −0.02 ± 0.14 (p = 0.67) for SVC. The measured (ΔSUV) and predictive ($\widetilde{\Delta SUV}$) changes are shown in Table 5. The relationship between measured and predicted SUVs is depicted in Fig. 4.

Model's reproducibility

Reproducibility was tested in 6 of the 15 patients (age: 58 ± 16.33, p = 0.40 compared to the derivation group) enrolled in the validation group. There were no differences with the derivation group in time interval between injection and acquisition, SUVmax and SUVmean [T1: 68.71 ± 9.54 min (p = 0.80), $SUVmax^{T1}$: 2.20 ± 0.19 (p = 0.27), $SUVmean^{T1}$: 1.42 ± 0.24 (p = 0.48), T2: 135.26 ± 24.10 min (p = 0.59), $SUVmax^{T2}$: 1.86 ± 0.22 (p = 0.53), $SUVmean^{T2}$: 1.06 ± 0.15 (p = 0.22)]. Figure 5 depicts the relationship between measured and predicted SUVs. Similar changes of the SUVs values were observed using our linear predictive model. Specifically, the differences between measured and predicted SUVs in the examined vascular segments were ASC: 0.004 ± 0.06 (p = 0.80), ARC: 0.01 ± 0.06 (p = 0.45), DSC: 0.02 ± 0.06 (p = 0.28), ABD: 0.02 ± 0.16 (p = 0.79) and SVC: 0.02 ± 0.16 (p = 0.79).

Discussion

In the present study we have demonstrated how aortic and SVC SUV change over time between T1 = 68.4 ± 8.9 min and T2 = 131.9 ± 20.8 min post-[^{18}F]FDG injection and in addition, we have developed a linear model allowing accurate and reproducible prediction of that change.

We have observed a decrease of SUV over time, both in the derivation and validation groups. This is in accordance with the findings of Bucerius et al. [17], who performed [^{18}F]FDG PET/CT imaging of the aorta in 195 patients. Regarding the relationship between time delay from tracer injection and aortic [^{18}F]FDG uptake values, significantly higher aortic SUVmax were observed at the earliest tertile (78–111) minutes between [^{18}F]FDG injection and acquisition time compared to the second tertile (111, 145) minutes. Similar are the observations by Cheng et al. [18] who studied 30 patients with [^{18}F]FDG PET/CT imaging at 1, 2 and 3 h after tracer injection. They found that [^{18}F]FDG activity (based on either SUVmean or SUVmax) in the aorta decreased significantly and continuously from 1 to 2 and from 2 to 3 h in all 30 patients.

Prior studies have used predictive models of tumor SUV change over time [10–12, 22–24]. Wong et al. [22] proposed a power function to approximate [^{18}F]FDG uptake over a limited time range. Complex methods of correcting [^{18}F]FDG uptake for different time intervals have been suggested [22–24]. Beaulieu et al. [10] reported that SUV in breast cancer changes in a linear fashion between approximately 30 to 75 min post-injection and developed a method by which users could correct SUVs for different time intervals between injection and acquisition. Their method relied on data that relate tumor SUVs

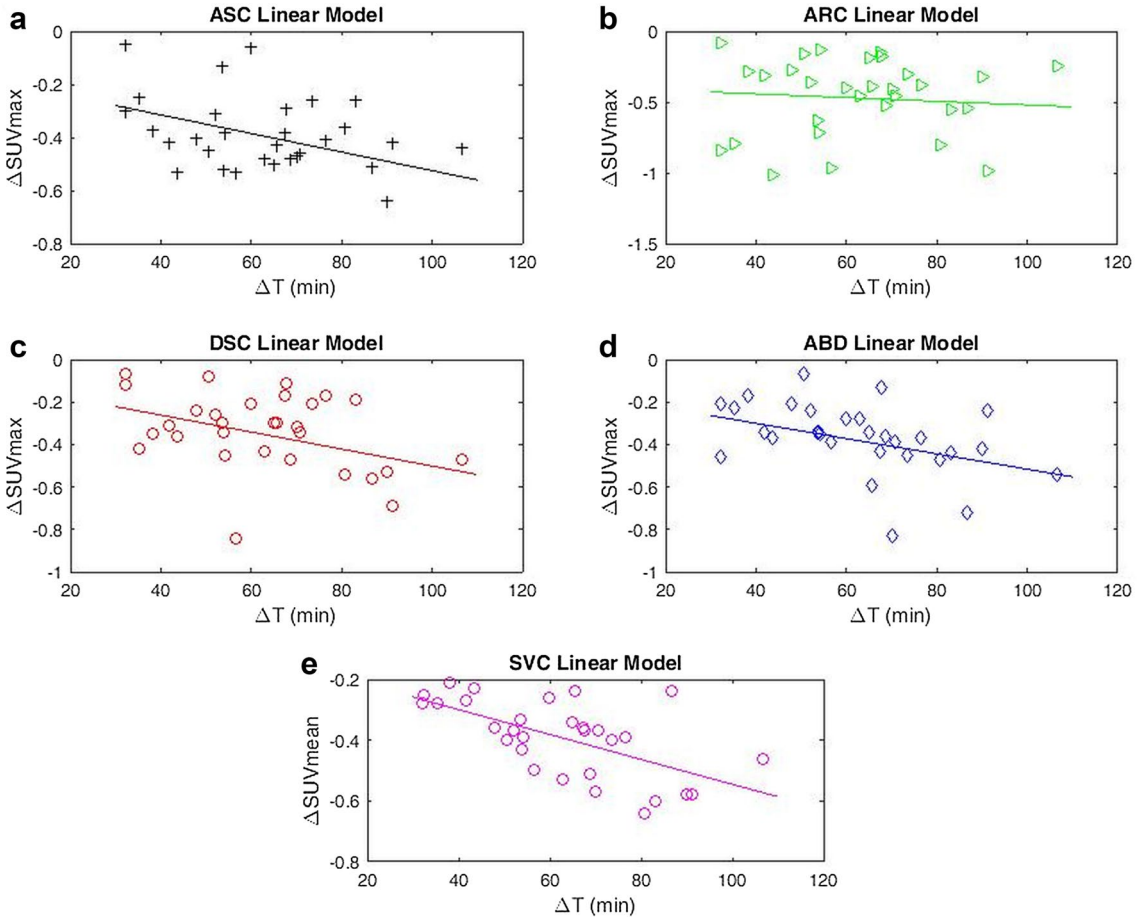

Fig. 2 Final predictive linear models (ΔT, ΔSUV) for **a** ASC, **b** ARC, **c** DSC, **d** ABD and **e** SVC. *ΔSUV* indicates the difference of standardized uptake value in T1 and T2, *ΔT* the difference time between the two scans, *ASC* ascending aorta, *ARC* aortic arch, *DSC* descending aorta, *ABD* abdominal aorta, *SVC* superior vena cava

at fixed time points after [^{18}F]FDG injection to a certain slope and intercept of SUV changes over time, allowing estimation of SUVs at different time points. The average percent error using the method to adjust for time differences was 8% and 5% for maximum SUVs and average SUVs respectively ranging from 2 to 12. Stahl et al. [11] simplified Beaulieu's method using a single reference point and implemented it in a patient cohort with breast cancer who were imaged from 63 ± 10 to 83 ± 10 min after [^{18}F]FDG injection to make appropriate time corrections for tumor SUVs. Results using the reference point method for time corrections are not different from the results using Beaulieu's method [10], because both methods were algebraically equivalent. In the study by Laffon et al. [12] a simple normalization of decay-corrected SUV for time differences after injection (within the 55- to 110-min) was proposed: $SUV_N = 1.66 * SUV_{uncorr}(t)$, where the factor 1.66 arose from decay correction at $t = 79$ min. No significant difference 0.04 ± 0.22 was found between the two uncorrected SUVs (SUV_N and SUV_{uncorr}). The simple SUV normalization was verified in patients with lung cancer, with a $\pm 2.5\%$ relative measurement uncertainty.

In contrast to the predicted models discussed above, our model is the first one predicting vascular SUV change over time, demonstrating very good reproducibility with only minor differences, likely of limited practical importance, between measured and predicted SUVs in the examined vascular segments. The changes of vessel [^{18}F]FDG uptake between $T1 = 68.4 \pm 8.9$ min and $T2 = 131.9 \pm 20.8$ min post-injection were well described by a linear fit. In contrast, the non-linear model did not exhibit the same performance. Although the wall of the aorta or the vena cava is substantially smaller compared to malignant lesions, the differences between measured and predicted values were very small and similar to those observed in prior studies from the oncology setting [10–12]. More importantly, the mean differences between measured and predicted values in our study are significantly lower than mean SUV differences between healthy individuals and patients with either established cardiovascular disease or with risk factors for atherosclerosis

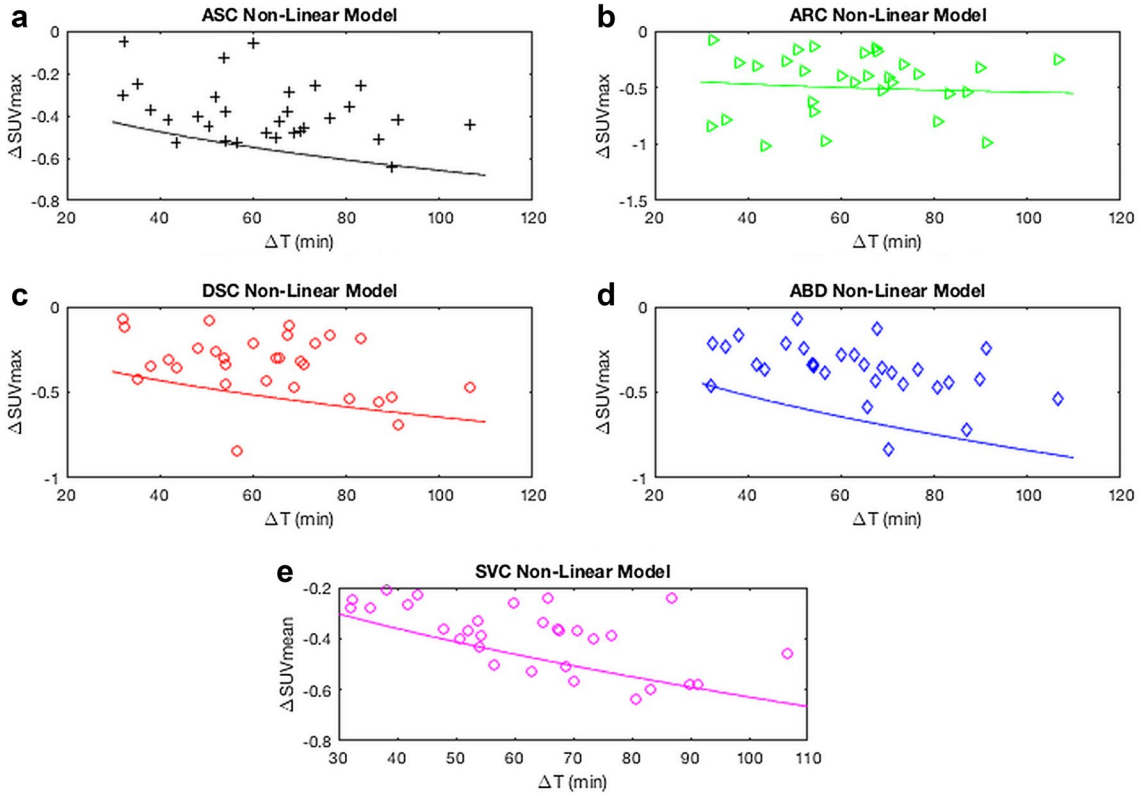

Fig. 3 Final predictive non-linear models (ΔT, ΔSUV) for **a** ASC, **b** ARC, **c** DSC, **d** ABD and **e** SVC. *ΔSUV* indicates the difference of standardized uptake value in T1 and T2, *ΔT* the difference time between the two scans, *ASC* ascending aorta, *ARC* aortic arch, *DSC* descending aorta, *ABD* abdominal aorta, *SVC* superior vena cava

Table 4 Measured and predictive reduction of SUV in the derivation group

Segment	Model	ΔSUV	$\widetilde{\Delta SUV}$	p
ASC	Linear	−0.38 ± 0.11	−0.39 ± 0.06	0.66
	Non-linear		−0.55 ± 0.06	< 0.05
ARC	Linear	−0.46 ± 0.13	−0.47 ± 0.03	0.90
	Non-linear		−0.50 ± 0.03	0.49
DSC	Linear	−0.34 ± 0.12	−0.35 ± 0.07	0.67
	Non-linear		−0.52 ± 0.07	< 0.05
ABD	Linear	−0.37 ± 0.12	−0.38 ± 0.07	0.67
	Non-linear		−0.65 ± 0.10	< 0.05
SVC	Linear	−0.39 ± 0.10	−0.39 ± 0.07	0.96
	Non-linear		−0.47 ± 0.09	< 0.05

All values are expressed as mean ± SD

ASC indicates ascending aorta, *ARC* aortic arch, *DSC* descending aorta, *ABD* abdominal aorta, *SVC* superior vena cava, *ΔSUV* the measured difference of standardized uptake value in T1 and T2, $\widetilde{\Delta SUV}$ the predictive difference of standardized uptake value in T1 and T2

Table 5 Measured and predictive reduction of SUV in the validation group

Segment	ΔSUV	$\widetilde{\Delta SUV}$	p
ASC	−0.40 ± 0.11	−0.40 ± 0.07	0.72
ARC	−0.45 ± 0.13	−0.47 ± 0.02	0.56
DSC	−0.33 ± 0.13	−0.35 ± 0.07	0.33
ABD	−0.41 ± 0.12	−0.38 ± 0.07	0.34
SVC	−0.41 ± 0.11	−0.39 ± 0.07	0.67

All values are expressed as mean ± SD

ASC indicates ascending aorta, *ARC* aortic arch, *DSC* descending aorta, *ABD* abdominal aorta, *SVC* superior vena cava, *ΔSUV* the measured difference of standardized uptake value in T1 and T2, $\widetilde{\Delta SUV}$ the predictive difference of standardized uptake value in T1 and T2

[25]. Interestingly, the aortic and vena cava SUV values at T2 in the derivation group of our study were very similar (1.92 ± 0.35 for ASC and 0.97 ± 0.17 for SVC respectively) to those reported by van der Valk [25] in their healthy control group (1.98 ± 0.31 and 0.96 ± 0.11 respectively), which was of similar age to that of our patients (60 ± 11 years).

Considering the variability of SUV between studies in the same patient [5–7, 19, 20], we focused our analysis only on individuals free of disease and by using the random sampling Monte Carlo Inversion Technique, we have tried to introduce this variability by simulating SUV values within a

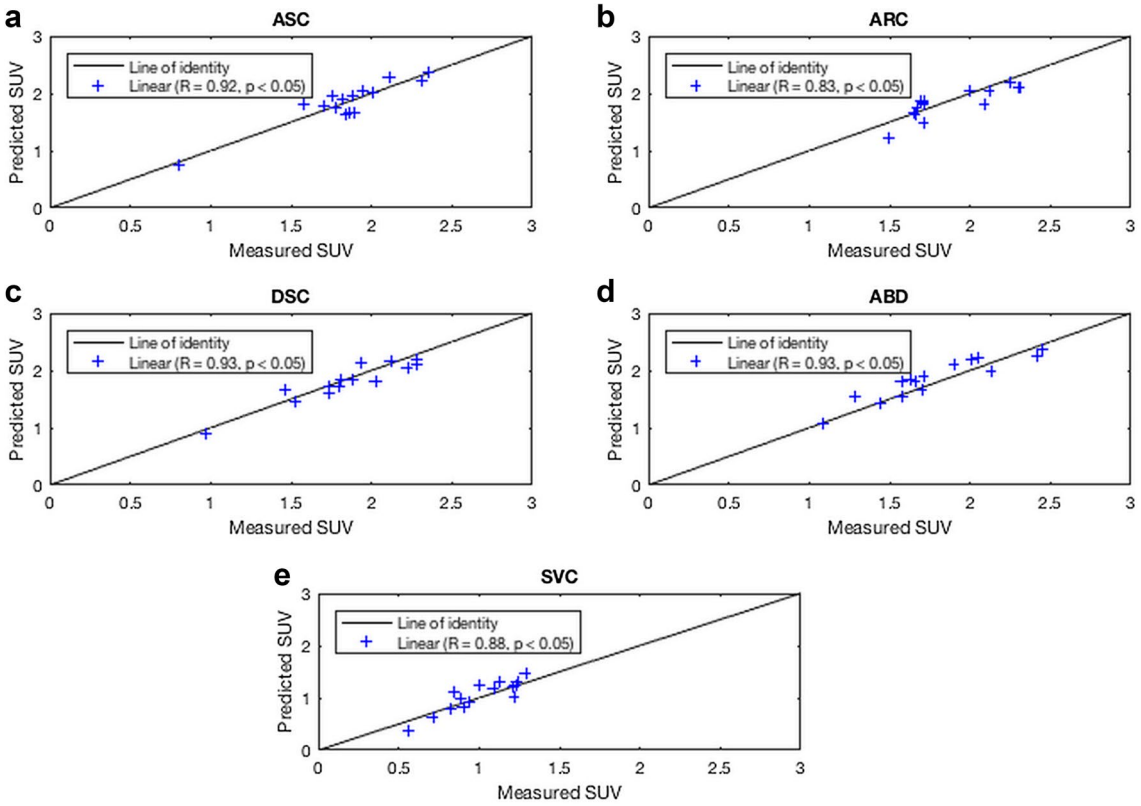

Fig. 4 Relationship between predicted SUV at T2 min after injection (using Eqs. 3 and 4) and measured value at T2 min for 15 patients of validation group in **a** ASC, **b** ARC, **c** DSC, **d** ABD and **e** SVC. *SUV* indicates standardized uptake value, *ASC* ascending aorta, *ARC* aortic arch, *DSC* descending aorta, *ABD* abdominal aorta, *SVC* superior vena cava

broader range for all the SUV measurements. In this way, we include SUV values within this range giving the model the ability to take into account the variability of the SUV. Thus, we populated our sample by generating 1000 (ΔT, $\widehat{\Delta SUV}$) points for each examined segment creating values that cover a broad range and increasing our statistics. Moreover, we repeated the procedure by shuffling our data and creating 100 different pairs of training/test sets keeping always the same proportion to reduce any statistical bias.

For quantitative assessment of possible arterial inflammation in a clinical or a research setting, acquisition of scans at 2–3 h post [^{18}F]FDG injection is recommended and ideally for interpretation of scan findings, comparisons should be made with a department's established SUV thresholds of normality. Considering that patients having dedicated vascular studies with delayed imaging constitute a small minority of the workload of most PET/CT departments, establishment of such thresholds may require acquisition of a second time-point delayed scan at 2–3 h post injection, in patients who have already undergone imaging for clinical purposes (e.g. patients investigated for potential malignancy with scans obtained at 60 min post-injection) and found to be disease-free. Our modeling approach may contribute to minimization of the sample size of a disease-free group of individuals and their exposure to radiation.

Limitations

The linear model was tested for SUV values ranging from 0.56 to 3.18 measured between $T1 = 68.4 \pm 8.9$ min and $T2 = 131.9 \pm 20.8$ min and, thus, our model may not apply to SUVs outside this range or outside the specified time interval. Also, our model assumes that the SUV curves are approximately linear within the specified time interval. Finally, as there is some variability in study protocols across different centers, our results can only be extrapolated to imaging studies obtained by a methodology that is similar to ours.

Conclusion

We have developed a predictive linear model of SUV changes in the aorta and SVC. This model demonstrates very good reproducibility with minor non-statistically significant

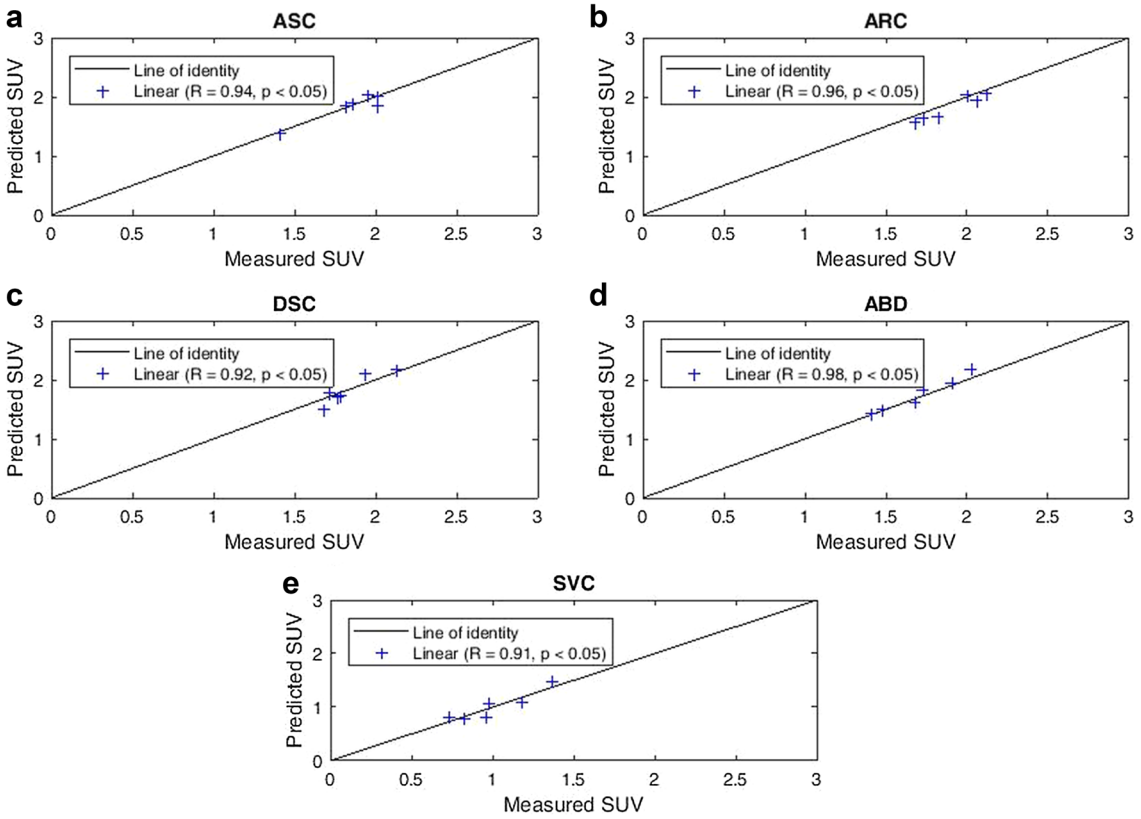

Fig. 5 Relationship between predicted SUV at T2 min after injection (using Eq. 3) and measured value at T2 min for the first 6 patients enrolled in the validation group in **a** ASC, **b** ARC, **c** DSC, **d** ABD and **e** SVC. *SUV* indicates standardized uptake value, *ASC* ascending aorta, *ARC* aortic arch, *DSC* descending aorta, *ABD* abdominal aorta, *SVC* superior vena cava

differences, likely of limited clinical importance, between measured and predicted SUVs.

Acknowledgements George M. Spyrou is funded by the European Commission Research Executive Agency Grant BIORISE (No. 669026), under the Spreading Excellence, Widening Participation, Science with and for Society Framework. Pavlos' Kafouris doctoral thesis is co-financed by Greece and the European Union (European Social Fund - ESF) through the Operational Programme «Human Resources Development, Education and Lifelong Learning» in the context of the project «Strengthening Human Resources Research Potential via Doctorate Research» (OPS-5003404), implemented by the State Scholarships Foundation (IKϒ).

Compliance with ethical standards

Conflict of interest The authors declare that they have no conflict of interest.

References

1. Dweck MR, Chow MW, Joshi NV, Williams MC, Jones C, Fletcher AM et al (2012) Coronary arterial 18F-sodium fluoride uptake: a novel marker of plaque biology. J Am Coll Cardiol 59:1539–1548
2. Menezes LJ, Kayani I, Ben-Haim S, Hutton B, Ell PJ, Groves AM (2010) What is the natural history of 18F-FDG uptake in arterial atheroma on PET/CT? Implications for imaging the vulnerable plaque. Atherosclerosis 211:136–140
3. Myers KS, Rudd JH, Hailman EP, Bolognese JA, Burke J, Pinto CA et al (2012) Correlation between arterial FDG uptake and biomarkers in peripheral artery disease. JACC Cardiovasc Imaging 5:38–45
4. Kang S, Kyung C, Park JS, Kim S, Lee SP, Kim MK et al (2014) Subclinical vascular inflammation in subjects with normal weight obesity and its association with body fat: an ^{18}F-FDG-PET/CT study. Cardiovasc Diabetol 13:70
5. Huet P, Burg S, Le Guludec D, Hyafil F, Buvat I (2015) Variability and uncertainty of 18F-FDG PET imaging protocols for assessing inflammation in atherosclerosis: suggestions for improvement. J Nucl Med 56:552–559
6. Paquet N, Albert A, Foidart J, Hustinx R (2004) Within-patient variability of (18)F-FDG: standardized uptake values in normal tissues. J Nucl Med 45:784–788
7. Keyes JW (1995) SUV: standard uptake or silly useless value? J Nucl Med 36:1836–1839
8. Boellaard R, Delgado-Bolton R, Oyen WJ, Giammarile F, Tatsch K, Eschner W et al (2015) FDG PET/CT: EANM procedure guidelines for tumour imaging: version 2.0. Eur J Nucl Med Mol Imaging 42:328–354
9. Bucerius J, Hyafil F, Verberne HJ, Slart RH, Lindner O, Sciagra R et al (2016) Position paper of the Cardiovascular Committee of the European Association of Nuclear Medicine (EANM) on

PET imaging of atherosclerosis. Eur J Nucl Med Mol Imaging 43:780–792
10. Beaulieu S, Kinahan P, Tseng J, Dunnwald LK, Schubert EK, Pham P et al (2003) SUV varies with time after injection in (18) F-FDG PET of breast cancer: characterization and method to adjust for time differences. J Nucl Med 44:1044–1050
11. Stahl AR, Heusner TA, Hartung V, Nagarajah J, Bockisch A, Hahn S et al (2011) Time course of tumor SUV in ^{18}F-FDG PET of breast cancer: presentation of a simple model using a single reference point for time corrections of tumor SUV. J Nucl Med 52:18–23
12. Laffon E, de Clermont H, Marthan R (2011) A method of adjusting SUV for injection-acquisition time differences in ^{18}F-FDG PET Imaging. Eur Radiol 21:2417–2424
13. Steyerberg EW, Harrell FE, Borsboom GJ, Eijkemans MJ, Vergouwe Y, Habbema JD (2001) Internal validation of predictive models: efficiency of some procedures for logistic regression analysis. J Clin Epidemiol 54:774–781
14. Kuncheva LI (2007) A stability index for feature selection. In: Proceedings of the 25th IASTED international multi-conference conference artificial intelligence and applications 2007, Innsbruck, Austria, Feb 12–14, pp 390–395
15. Toutouzas K, Koutagiar I, Benetos G, Aggeli C, Georgakopoulos A, Athanasiadis E et al (2017) Inflamed human carotid plaques evaluated by PET/CT exhibit increased temperature: insights from an in vivo study. Eur Heart J Cardiovasc Imaging 18:1236–1244
16. Brili S, Oikonomou E, Antonopoulos AS, Pianou N, Georgakopoulos A, Koutagiar I et al (2018) 18F-fluorodeoxyglucose positron emission tomography/computed tomographic imaging detects aortic wall inflammation in patients with repaired coarctation of aorta. Circ Cardiovasc Imaging 11:e007002
17. Bucerius J, Mani V, Moncrieff C, Machac J, Fuster V, Farkouh ME et al (2014) Optimizing ^{18}F-FDG PET/CT imaging of vessel wall inflammation—the impact of ^{18}F-FDG circulation time, injected dose, uptake parameters, and fasting blood glucose levels. Eur J Nucl Med Mol Imaging 41:369–383
18. Cheng G, Alavi A, Lim E, Werner TJ, Del Bello CV, Akers SR (2013) Dynamic changes of FDG uptake and clearance in normal tissues. Mol Imaging Biol 15:345–352
19. Kinahan P, Fletcher J (2010) PET/CT standardized uptake values (SUVs) in clinical practice and assessing response to therapy. Semin Ultrasound CT MR 31:496–505
20. Boellaard R (2009) Standards for PET image acquisition and quantitative data analysis. J Nucl Med 50(Suppl 1):11S–20S
21. Hagiwara K (2002) Review of particle properties. Phys Rev D 66:010001(R)
22. Wong CY, Noujaim D, Fu HF, Huang WS, Cheng CY, Thie J et al (2009) Time sensitivity: a parameter reflecting tumor metabolic kinetics by variable dual-time F-18 FDG PET imaging. Mol Imaging Biol 11:283–290
23. Thie AJ (2004) Understanding the standardized uptake value, its methods, and implications for usage. J Nucl Med 45:1431–1434
24. Thie AJ, Hubner FK, Smith TG (2002) Optimizing imaging time for improved performance in oncology PET studies. Mol Imaging Biol 4:238–244
25. van der Valk FM, Verweij SL, Zwinderman KA, Strang AC, Kaiser Y, Marquering HA et al (2016) Thresholds for arterial wall inflammation quantified by 18F-FDG PET imaging: implications for vascular interventional studies. JACC Cardiovasc Imaging 9:1198–1207